Investigation on the Physics of Temporal Heat Transfer Behavior in Unsteady Conjugated Heat Transfer Processes

By C. L. Liu & J. von Wolfersdorf†

School of Power and Energy, Northwestern Polytechnical University,You Yi Xi Lu 127, 710072 Xi'an, China

†Institute of Aerospace Thermodynamics, University of Stuttgart, Pfaffenwaldring 31, 70569 Stuttgart, Germany

Numerical simulations with unsteady RANS method have been performed to reveal the physics of unsteady behavior of heat transfer coefficient observed in conjugated heat transfer experiment under steady flow velocity and unsteady flow temperature. Unconjugated model with different wall thermal boundary conditions have also been computed to help to identify the reason. The results show that the conventionally defined heat transfer coefficient $h_{Tg}(\tau)$ with the flow temperature in the mainstream region pulsates intensely with the pulsating flow temperature. The pulsating amplitude of $h_{Tg}(\tau)$ is different under different wall thermal boundary conditions. When the flow temperature is unsteady, there is phase shift between local adiabatic wall temperature $T_{aw}(\tau)$ and flow temperature in the mainstream region $T_g(\tau)$ due to the velocity difference between mainstream and boundary layer. When the local adiabatic wall temperature is used to define the heat transfer coefficient $h_{Taw}(\tau)$, it can exclude the influence of unsteady flow temperature and make the $h_{Taw}(\tau)$ be a good invariant descriptor in heat transfer with steady flow velocity and unsteady flow temperature. The temporal behavior of $h_{Taw}(\tau)$ is determined by the temporal behavior of heat flux boundary condition on the wall. And detailed analysis has been provided.

1. Introduction

In the field of heat transfer research, unsteady forced convection represents a topic of much interest in many thermal systems, such as regenerative heat exchangers, nuclear reactor fuel rods and turbomachines. They are often subjected to time varying thermal boundary conditions, for instance, periodically varying flow temperatures. Knowledge of the unsteady heat transfer in a steady flow with periodically varying flow temperature is important for many engineering applications where hot and cold fluids pass in succession.

In analyzing thermal responses of solid surfaces interacting with a steady flow of unsteady flow temperature, it is common to assume that quasi-steady conditions prevail, meaning that at every instant of time the heat convection experiences an instantaneous steady state and is basically determined by the flow conditions and less influenced due to variations in flow temperature. From the standpoint of practical computations, the quasi-steady approach utilizes a steady-state heat transfer coefficient to the transient conjugated convection process. Many studies use this assumption for turbulent flows but question it for the laminar case. Therefore, numerous investigations were carried out to check up the validation of the quasi-steady assumption in laminar flow conditions. Sparrow and De Farias [1] are probably the first to study the effect of time varying inlet temperature conditions on the conjugated, laminar convection of a steady slug flow in a flat plate channel. Comparisons between the quasi-steady approach result and numerical solutions showed the validation of the quasi-steady approach for a range of operating conditions. Sucec [2] describes an exact solution for the transient, conjugated, laminar convection problem consisting of a plate interacting with a steady flow whose temperature varied sinusoidally with time. Comparison of the exact solution with the quasi-steady approach indicated acceptable agreement at some conditions and inadequate accuracy in predicting time varying wall temperature in general. To address this problem, Sucec [3] proposed an improved quasi-steady approach for transient, conjugated, laminar convection problems of steady flows with time varying temperature. The comparisons showed that it performed much better than the standard quasi-steady approach. Recently, Hadiouche and Mansouri [4] studied the unsteady conjugated heat transfer for a fully developed laminar steady flow with periodically varying inlet temperature. An exact solution was presented. The results showed that the instantaneous Nusselt number becomes highly time-dependent under higher flow temperature frequency and the quasi-steady approach is inadequate. Other studies on the transient conjugated convection of laminar steady flow with time varying temperature can be found in [5–8]. Those studies addressed the problem with analytical or numerical methods, and the behavior of periodic responses, including amplitudes and phase lags of oscillations in the wall temperature, flow bulk temperature and heat flux, was investigated. For all the above conjugated convection studies, lumped capacity method is always used based on simplified conjugated models, for example, a thin plate without conduction inside. Due to that the quasi-steady assumption is commonly accepted by researchers for turbulent flows, there are relatively fewer investigations on the conjugated convection problem for steady turbulent flows with time varying temperatures. The performed investigations on this topic mainly paid attention on the behavior of periodic responses. Kim and Özisik [9] developed a method to analyze the turbulent forced convection inside a parallel-plate channel with a periodically varying flow temperature and a uniform constant wall temperature. The variation of the amplitudes and phase lag of both fluid bulk temperature and the wall heat flux along the channel was investigated. Kakac and Li [10] presented a theoretical and experimental study of turbulent forced convection subjected to a sinusoidally varying flow temperature. Analytical solutions were compared with the experimental findings and a satisfactory agreement was obtained. The effects of the modified Biot number, the fluid-to-wall thermal capacitance ratio and the Reynolds number on the temperature amplitude along the channel were discussed. In Kakac and Li [10], the effect of the wall thermal capacitance was considered by using simplified conjugated models which, however, did not take the conduction inside the wall into account. the effect of the wall thermal capacitance was considered by using simplified conjugated models which, however, did not take the conduction inside the wall into account. In Arik et al. [11], the heat transfer characteristics of the turbulent flow with periodically varying temperature were determined for linear varying wall temperature and constant wall temperature boundary conditions. Experiments were also performed to validate the employed mathematical modeling and to compare it with the analytical solutions.

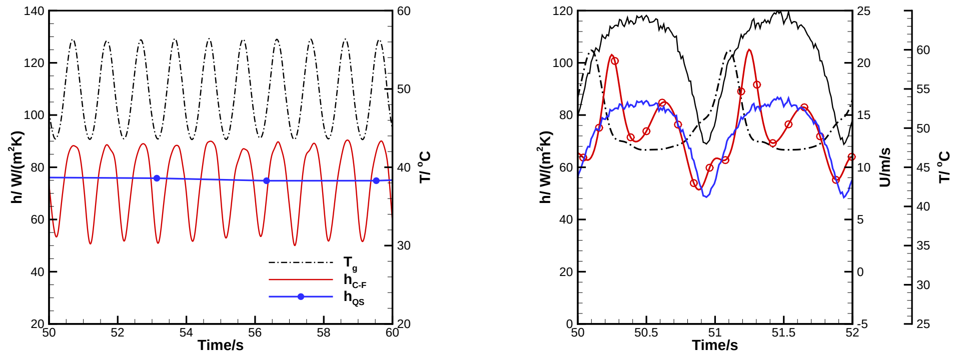

(a) Steady turbulent flow with periodically pulsating flow temperature [12]

(b) Periodically pulsating turbulent flow with time varying flow temperature [14]

FIGURE 1. Time-resolved experimental results of heat transfer at one measurement point under periodic aero-thermal conditions with a frequency of 1Hz

With the sponsorship from Alexander von Humboldt Foundation of Germany, the authors systematically performed experimental investigations on the time-resolved characteristics of heat transfer under periodically unsteady aero-thermal conditions. A simple rectangular channel model was investigated to exclude the influence of other complications. Detailed instantaneous behavior of heat transfer coefficient was measured for conditions of steady flow with periodically pulsating flow temperatures [12,13] and periodically pulsating flows with time varying flow temperatures [14]. Experimental results of one case for each unsteady aero-thermal condition are shown in Fig. 1, in which h$_{C-F}$ is the heat transfer coefficient measured with method without quasi-steady restriction; h$_{QS}$ is the heat transfer coefficient measured with method based on quasi-steady hypothesis; h$_{QS-COR}$ is the heat transfer coefficient calculated with the instantaneous flow velocity and quasi-steady empirical correlation; T$_g$ and U$_g$ are the flow temperature and velocity respectively. The measured results show that whether the flow velocity is steady or not, the heat transfer coefficient can be dramatically influenced by the unsteady flow temperatures, especially when the boundary layer is turbulent. The temporal behavior of those measured heat transfer coefficient is contrary to the quasi-steady hypothesis that heat transfer coefficient is only determined by the instantaneous flow velocity and could not be influenced by the flow temperature unsteadies. Therefore, more and deeper analysis is necessary for the clarification of the physics of temporal heat transfer behavior in the unsteady conjugated heat transfer processes.

Based on the experimental work performed by the authors at ITLR, detailed unsteady numerical simulations with RANS have been carried out to reveal the physics of unusual temporal behaviour of heat transfer coefficient related to the experimental situations. Unconjugated model will also be computed and compared to the conjugated model to identify the reason for the temporal behavior of heat transfer coefficient.

2. Numerical simulation approach

2.1. *Computational model and discretization*

The computational model was built according to the test channel size introduced in [12]. The trip wire was simulated in the computational model with a small square, which had the same hydraulic diameter as the real trip wire for an easy block-structured mesh generation. The computation model, which is illustrated in Fig. 2(a), is a two-dimensional model in which the symmetry condition is used to reduce the domain to one half of the test channel height.

The computational domain was discretized by a block-structured grid with quadrilateral cells, which applies to both the fluid and the solid region. Grid dependence studies were performed with four sets of grids. Three of those four had the same grid density in the solid zone but different grid densities in the fluid zone. The cell number was about 19 thousand in the solid zone and about 40 thousand, 70 thousand and 79 thousand respectively in the fluid zone for the three cases. Compared with the results from the fine grid, the difference in calculated heat transfer coefficients at P1 was about 3% for the coarse grid and less than 1% for the intermediate grid. When the cell number in the solid zone was increased to 31 thousand, the differences in the calculated heat transfer coefficients were so small that can be neglected. Therefore, grid-independent results can be obtained with a total cell number of about 89 thousand. In this grid system, the y^+ value at the wall-adjacent cell was kept to be in the order of 1 and an increment ratio of 1.15 was set for the boundary layer mesh to meet the requirement of the chosen turbulence model to resolve the details in the viscosity-affected near-wall region. A close-up of the local grid of the computational model is shown in Fig. 2(b). For unconjugated computational model, the only difference from conjugated model is that the solid zone was removed. In the present study, temporal behavior of heat transfer coefficient at P1, which is 160mm from the leading edge of the solid zone, was analyzed.

2.2. *Solver*

The commercial CFD solver FLUENT (version 13.0) was used to solve the two dimensional unsteady Reynolds-averaged Navier-Stokes equations coupling with the unsteady heat conduction in the solid zone as a transient conjugated problem. The commonly used and validated SST $k - \omega$ turbulence model with low-Re corrections, which can resolve the details in the viscous sublayer by applying very fine mesh length scales near the walls, was selected in the present study. The turbulent Prandtl number Pr_t which is used to model the turbulent heat diffusion was set as the commonly used constant value of 0.85. A second order implicit time stepping formulation was used for the temporal discretization of the transient terms. The discretization scheme for the convection terms was the QUICK scheme which is of third order precision for structural quadrilateral meshes. The velocity-pressure coupling was achieved by using the well-known SIMPLEC algorithm. The equations of mass, momentum, energy and turbulence were solved sequentially with an implicit procedure algorithm at every time step. Convergence was determined based on drop in normalized residuals by four orders of magnitude (10^{-4}) for the mass, momentum and turbulence parameter equations and by nine orders of magnitude (10^{-9}) for the energy equation. The algebraic multi-grid method was employed to speed up the converging process.

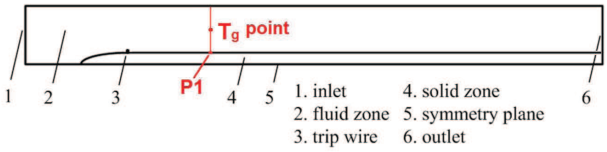

(a) Computational model geometry

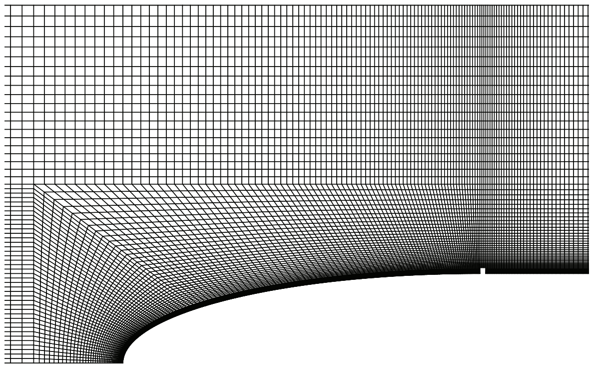

(b) Local grids in fluid zone

FIGURE 2. Computational model geometry and local grid details

2.3. *Boundary conditions*

At the channel inlet, a steady and uniform bulk velocity was prescribed to make the velocity in the mainstream region at P1 be 21 m/s which is the same with the velocity in experiment [12]. Turbulence intensity for the incoming flow was set to 1.3%. Two cases with the same flow velocity condition but different flow temperature conditions were simulated. One is constant flow temperature. And the other is unsteady flow temperature which pulsated sinusoidally with a mean temperature of 323K and pulsation amplitude of 12K. At the outlet, a constant pressure boundary condition was prescribed. All walls were modeled as no-slip walls. For conjugate heat transfer computations, the solid zone, which is the test plate, was modeled with the same properties ρ_w, c_w, k_w for Perspex. Symmetry condition was applied on the centerline plane of the two-dimensional computational model. For unconjugated heat transfer computations, two types of boundary condition were set on the wall. One is the temperature boundary condition (Dirichlet boundary condition). And the other is the heat flux boundary condition (Neumann boundary condition). For the thermal properties of the air flow, including density, conductivity, specific heat capacity, constant values were assigned. Although this setting deviates from the reality, it can exclude the influence of varying thermal properties caused by unsteady flow temperature on the temporal behavior of heat transfer coefficient.

3. Results and analysis

We used two types of defination of heat transfer coefficient. One uses the flow temperature in the mainstream region, which was taken at "Tg point" shown in Fig. 2(a), as the reference temperature as Eq. (3.1):

$$h_{T_g}(\tau) = \frac{q(\tau)}{T_g(\tau) - T_w(\tau)} \tag{3.1}$$

The other uses the local adiabatic wall temperature under the same flow and temperature condition as the reference temperature as Eq. (3.2):

$$h_{T_{aw}}(\tau) = \frac{q(\tau)}{T_{aw}(\tau) - T_w(\tau)} \tag{3.2}$$

The first definition can be regarded as a conventional definition. And the second definition is preferred and regarded as a good invariant descriptor in complex heat transfer situations by researchers due to its sound physical basis introduced in Moffat [15].

When the flow temperature is steady, there is $T_{aw} = T_g$ and $h_{Taw}(\tau) = h_{Tg}(\tau)$. Fig. 3 shows that heat transfer coefficient of conjugated model is not steady under steady flow temperature. It increases from the value of heat transfer coefficient under constant T_w to the value of heat transfer coefficient under constant q_w. Constant T_w or q_w means that T_w or q_w is temporally steady and spatially uniform. For the conjugated model, both T_w and q_w at P1 was time-varying because the initial temperature of solid zone was different from the flow temperature. For the other two cases with constant T_w and q_w boundary condition respectively, heat transfer coefficient was constant. But it is not possible to identify whether the constant T_w boundary or the constant q_w boundary plays the key role because both T_w and q_w at P1 was constant under steady flow temperature for the two cases.

Fig. 4 to Fig. 6 respectively show the temporal behavior of heat transfer coefficient at P1 for conjugated model and unconjugated model with constant T_w and q_w boundary conditions under unsteady flow temperature. The figure in the left shows the varying trend in whole history, and the figure in the right shows the detailed temporal behavior in a short partial period. We can see that the conventionally defined heat transfer coefficient with Eq. (3.1) pulsates intensely with the pulsating flow temperature. It means that this conventional definition is not a good invariant descriptor in heat transfer with steady flow velocity and unsteady flow temperature. When the flow temperature is unsteady, there is a small phase shift between $T_{aw}(\tau)$ and $T_g(\tau)$ as shown in Fig. 4 to Fig. 6 due to the velocity difference between mainstream and boundary layer. When the local adiabatic wall temperature is used to define the heat transfer coefficient, we can see that $h_{taw}(\tau)$ becomes steady for the unconjugated model with constant q_w boundary condition. And the value of $h_{taw}(\tau)$ is equal to that under steady flow temperature and constant q_w boundary condition shown in Fig. 3. But for the other two models, $h_{taw}(\tau)$ still pulsates with the flow temperature, though the pulsating amplitude becomes smaller than $h_{tg}(\tau)$. These results indicate that $T_{aw}(\tau)$ can exclude the influence of unsteady flow temperature and make the $h_{taw}(\tau)$ be a good invariant descriptor in heat transfer with steady flow velocity and unsteady flow temperature when the wall is assigned constant q_w boundary condition which is temporally steady and spatially uniform.

Fig. 7 shows the temporal behavior of heat transfer coefficient at P1 for unconjugated model with steady but nonuniform q_w boundary conditions under steady and unsteady flow temperatures respectively. Comparison between Fig. 3 and Fig. 7 shows that the spatial distribution of q_w can influence the mean value of heat transfer coefficient. But under this condition, $T_{aw}(\tau)$ still can exclude the influence of unsteady flow temperature and make the $h_{Taw}(\tau)$ be a good invariant descriptor which has the same value with that under steady flow temperature as shown Fig. 7. Therewith, if we combine the unsteady

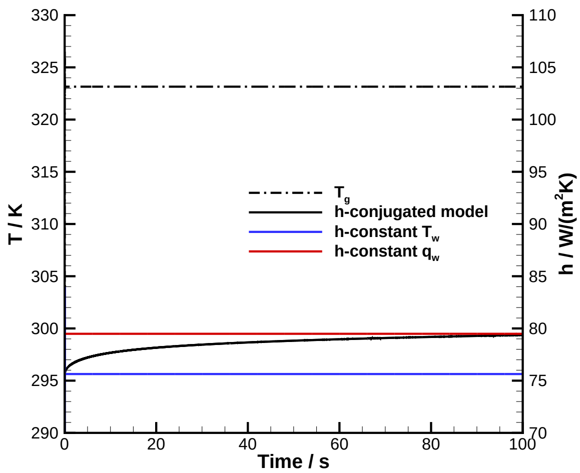

FIGURE 3. Time-resolved numerical results of heat transfer coefficients at P1 under different thermal boundary conditions with steady flow temperature

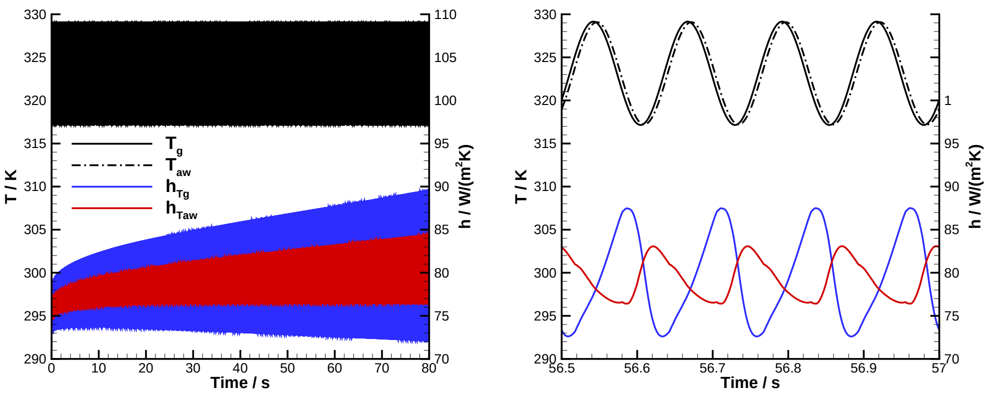

FIGURE 4. Time-resolved numerical results of heat transfer coefficients at P1 for conjugated model under unsteady flow temperature

$h_{Taw}(\tau)$ results for the conjugated model and unconjugated model with constant T_w boundary condition, in which the q_w in the upstream region of P1 is temporally unsteady and spatially nonuniform under unsteady flow temperatures, we can get a deduction that the temporally unsteady q_w boundary condition is the reason for the unsteady behavior of $h_{Taw}(\tau)$. And the T_w boundary condition cannot influence the temporal behavior of $h_{Taw}(\tau)$ because for case of constant q_w boundary condition with unsteady flow temperature the T_w is unsteady, while the $h_{Taw}(\tau)$ is steady.

To further verify this deduction, numerical simulations with unsteady but uniform q_w boundary condition expressed by Eq. (3.3) were performed under steady and unsteady

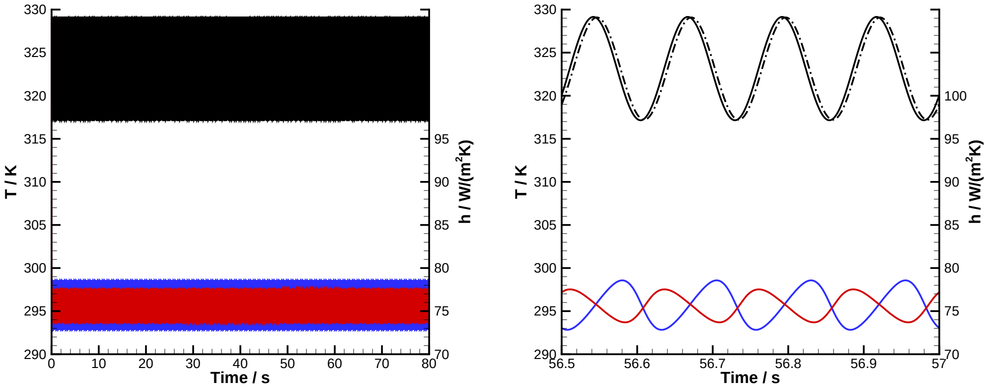

FIGURE 5. Time-resolved numerical results of heat transfer coefficients at P1 for constant wall temperature boundary condition under unsteady flow temperature

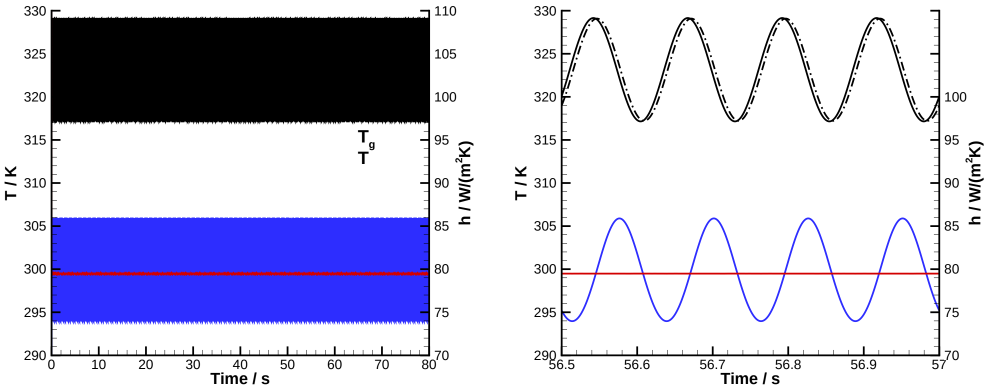

FIGURE 6. Time-resolved numerical results of heat transfer coefficients at P1 for constant heat flux boundary condition under unsteady flow temperature

flow

$$q_w\left(x,\tau\right) = \left[-2000 - 1000\sin\left(16\pi\cdot\tau\right)\right] \text{W/m}^2 \tag{3.3}$$

temperatures respectively. The results are shown in Fig. 8. We can see that the unsteady q$_w$ boundary condition can make the heat transfer coefficient pulsate intensely under steady flow temperature. It means that the temporal behavior of q$_w$ boundary condition, but not flow temperature, is the fundamental cause for the temporal behavior of heat transfer coefficient. When the flow temperature is unsteady, $T_{aw}(\tau)$ can exclude the influence of unsteady flow temperature and make the $h_{Taw}(\tau)$ act the same as the heat transfer coefficient under steady flow temperature with the same q$_w$ boundary condition.

The reason for the temporal behavior of $h_{Taw}(\tau)$ at P1 can be found in the spatial distribution of "Unsteady-term" at P1 which is defined as Eq. (3.4). Fig. 9 shows the

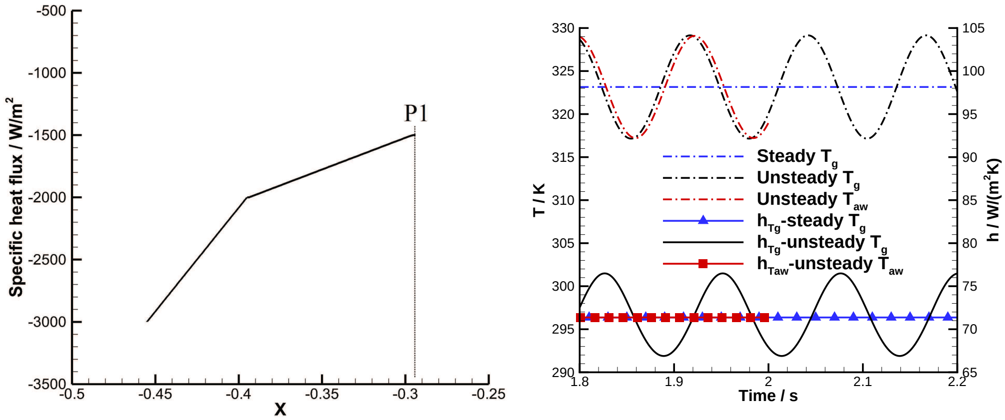

(a) Heat flux distribution upstream of P1 (b) Heat transfer results

FIGURE 7. Time-resolved numerical results of heat transfer coefficients at P1 for steady but nonuniform heat flux boundary condition

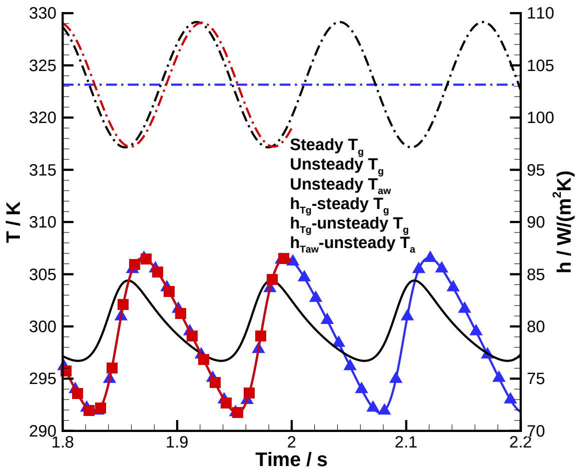

FIGURE 8. Time-resolved numerical results of heat transfer coefficients at P1 for unsteady but uniform heat flux boundary condition

spatial

$$\text{Unsteady-term} = \left.\frac{\partial T(\tau, y)}{\partial \tau}\right|_{\tau_0}^{x=\text{P1}} \tag{3.4}$$

distributions of "Unsteady-term" in y direction, which is normal to the wall, at P1 for cases under unsteady flow temperature with different wall thermal boundary conditions at twotime points. We can see that for the case with unsteady flow temperature and constant T_w boundary condition in which the q_w is unsteady, there is notable difference in the "Unsteady-term" distribution from the adiabatic case in the near-wall region at the same time point. But for the other cases with steady q_w boundary conditions, they have

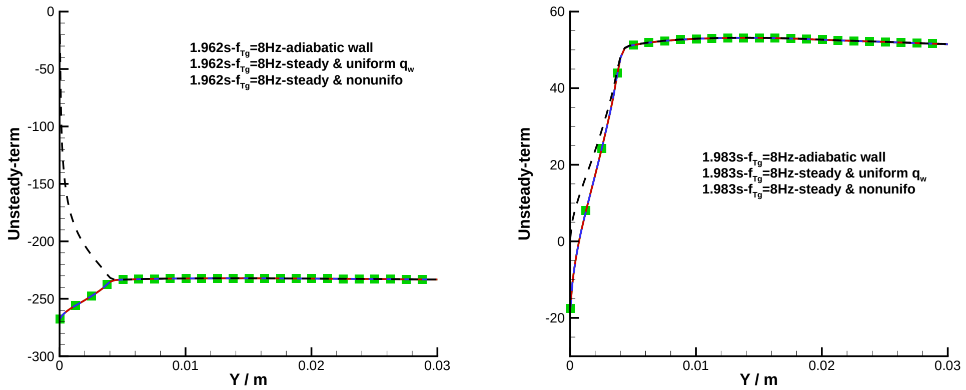

FIGURE 9. Spatial distribution of "Unsteady-term" in y direction at P1 for cases with different wall thermal boundary conditions

the same spatial distribution of "Unsteady-term" with the adiabatic case, no matter the q$_w$ distribution is uniform or nonuniform. Then the temporal behavior of $h_{Taw}(\tau)$ under steady q$_w$ boundary condition can be derived from this characteristic of "Unsteady-term":

$$
\begin{aligned}
&\frac{\partial T(\tau,y)}{\partial \tau}\bigg|_{T_g(\tau),q_w(x)}^{x=\mathrm{P1}} = \frac{\partial T(\tau,y)}{\partial \tau}\bigg|_{T_g(\tau),adiabatic}^{x=\mathrm{P1}}\\
&\Rightarrow \frac{\partial T_w(\tau)}{\partial \tau}\bigg|_{T_g(\tau),q_w(x)}^{x=\mathrm{P1},y=0} = \frac{\partial T_{aw}(\tau)}{\partial \tau}\bigg|_{T_g(\tau)}^{x=\mathrm{P1},y=0}\\
&\Rightarrow \frac{\partial (T_{aw}(\tau)-T_w(\tau))}{\partial \tau}\bigg|_{T_g(\tau),q_w(x)}^{x=\mathrm{P1}} = 0 = \frac{\partial (T_g-T_w)}{\partial \tau}\bigg|_{T_g,q_w(x)}^{x=\mathrm{P1}}\\
&\Rightarrow \frac{q_w}{(T_{aw}(\tau)-T_w(\tau))}\bigg|_{T_g(\tau),q_w(x)}^{x=\mathrm{P1}} = \frac{q_w}{(T_g-T_w)}\bigg|_{T_g,q_w(x)}^{x=\mathrm{P1}} = \frac{q_w}{(T_{aw}-T_w)}\bigg|_{T_g,q_w(x)}^{x=\mathrm{P1}}\\
&\Rightarrow h_{T_{aw}}(\tau)\big|_{T_g(\tau),q_w(x)}^{x=\mathrm{P1}} = \text{constant} = h_{T_g}\big|_{T_g,q_w(x)}^{x=\mathrm{P1}} = h_{T_{aw}}\big|_{T_g,q_w(x)}^{x=\mathrm{P1}}
\end{aligned}
$$

Fig. 10 shows the spatial distributions of "Unsteady-term" at P1 for cases with unsteady heat flux boundary condition. For the case with unsteady flow temperature and unsteady q$_w$ boundary condition, its "Unsteady-term" distribution is different from the adiabatic case in the near-wall region. As shown in Fig. 10, the "Unsteady-term" of steady flow temperature case is not zero in the near-wall region when the q$_w$ is unsteady. And the "Unsteady-term" of unsteady flow temperature case minus the "Unsteady-term" of steady flow temperature case is equal to the "Unsteady-term" of adiabatic wall case. Then the temporal behavior of $h_{Taw}(\tau)$ under unsteady q$_w$ boundary condition can be derived:

$$
\begin{aligned}
&\frac{\partial T(\tau,y)}{\partial \tau}\bigg|_{T_g(\tau),q_w(x,\tau)}^{x=\mathrm{P1}} - \frac{\partial T(\tau,y)}{\partial \tau}\bigg|_{T_g,q_w(x,\tau)}^{x=\mathrm{P1}} = \frac{\partial T(\tau,y)}{\partial \tau}\bigg|_{T_g(\tau),adiabatic}^{x=\mathrm{P1}}\\
&\Rightarrow \frac{\partial T(\tau,y=0)}{\partial \tau}\bigg|_{T_g(\tau),q_w(x,\tau)}^{x=\mathrm{P1}} - \frac{\partial T(\tau,y=0)}{\partial \tau}\bigg|_{T_g,q_w(x,\tau)}^{x=\mathrm{P1}} = \frac{\partial T(\tau,y=0)}{\partial \tau}\bigg|_{T_g(\tau),adiabatic}^{x=\mathrm{P1}}
\end{aligned}
$$

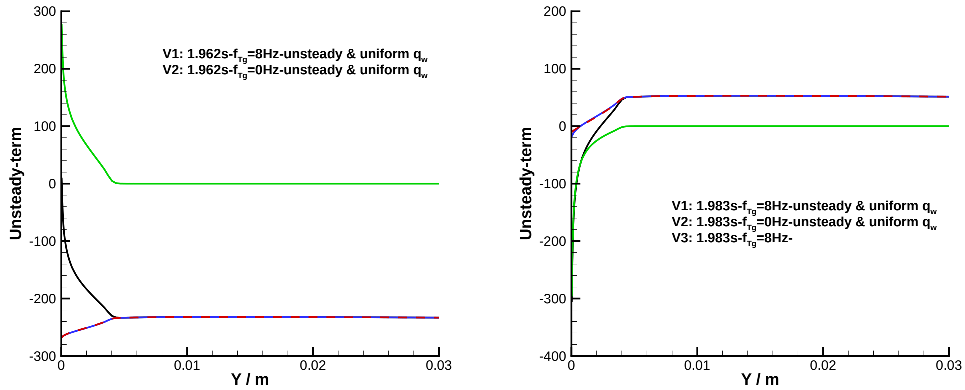

FIGURE 10. Spatial distribution of "Unsteady-term" in y direction at P1 for cases with unsteady heat flux boundary condition

$$\Rightarrow \left.\frac{\partial T_w(\tau)}{\partial \tau}\right|_{T_g(\tau),q_w(x,\tau)}^{x=\mathrm{P1}} - \left.\frac{\partial T_w(\tau)}{\partial \tau}\right|_{T_g,q_w(x,\tau)}^{x=\mathrm{P1}} = \left.\frac{\partial T_{aw}(\tau)}{\partial \tau}\right|_{T_g(\tau)}^{x=\mathrm{P1}}$$

$$\Rightarrow 0 - \left.\frac{\partial T_w(\tau)}{\partial \tau}\right|_{T_g,q_w(x,\tau)}^{x=\mathrm{P1}} = \left.\frac{\partial T_{aw}(\tau)}{\partial \tau}\right|_{T_g(\tau)}^{x=\mathrm{P1}} - \left.\frac{\partial T_w(\tau)}{\partial \tau}\right|_{T_g(\tau),q_w(x,\tau)}^{x=\mathrm{P1}}$$

$$\Rightarrow \left.\frac{\partial T_g}{\partial \tau}\right|_{T_g}^{x=\mathrm{P1}} - \left.\frac{\partial T_w(\tau)}{\partial \tau}\right|_{T_g,q_w(x,\tau)}^{x=\mathrm{P1}} = \left.\frac{\partial T_{aw}(\tau)}{\partial \tau}\right|_{T_g(\tau)}^{x=\mathrm{P1}} - \left.\frac{\partial T_w(\tau)}{\partial \tau}\right|_{T_g(\tau),q_w(x,\tau)}^{x=\mathrm{P1}}$$

$$\Rightarrow \left.\frac{\partial (T_{aw}(\tau)-T_w(\tau))}{\partial \tau}\right|_{T_g(\tau),q_w(x,\tau)}^{x=\mathrm{P1}} = \left.\frac{\partial (T_g-T_w(\tau))}{\partial \tau}\right|_{T_g,q_w(x,\tau)}^{x=\mathrm{P1}}$$

$$\Rightarrow \left(T_{aw}(\tau) - T_w(\tau)\right)\Big|_{T_g(\tau),q_w(x,\tau)}^{x=\mathrm{P1}} = \left(T_{aw} - T_w(\tau)\right)\Big|_{T_g,q_w(x,\tau)}^{x=\mathrm{P1}}$$

$$\Rightarrow \left.\frac{q_w(\tau)}{(T_{aw}(\tau)-T_w(\tau))}\right|_{T_g(\tau),q_w(x,\tau)}^{x=\mathrm{P1}} = \left.\frac{q_w(\tau)}{(T_g-T_w(\tau))}\right|_{T_g,q_w(x,\tau)}^{x=\mathrm{P1}} = \left.\frac{q_w(\tau)}{(T_{aw}-T_w(\tau))}\right|_{T_g,q_w(x,\tau)}^{x=\mathrm{P1}}$$

$$\Rightarrow h_{T_{aw}}(\tau)\Big|_{T_g(\tau),q_w(x,\tau)}^{x=\mathrm{P1}} = h_{T_g}(\tau)\Big|_{T_g,q_w(x,\tau)}^{x=\mathrm{P1}} = h_{T_{aw}}(\tau)\Big|_{T_g,q_w(x,\tau)}^{x=\mathrm{P1}}$$

References

[1] E. M. SPARROW, F. N. DE FARIAS. (1968). Unsteady heat transfer in ducts with time varying inlet temperature and participating walls. *Int. J. Heat Mass Transfer*. **11**, 837-853.

[2] J. SUCEC. (1980). Transient heat transfer between a plate and a fluid whose temperature varies periodically with time. *J. Heat Trans.-T. ASME*. **102**, 26-131.

[3] J. SUCEC. (1981). An improved quasi-steady approach for transient conjugate forced convection problems. *JInt. J. Heat Mass Transfer*. **24**, 1711-1722.

[4] A. HADIOUCHE AND K. MANSOURI. (2010). Analysis of the effects of inlet temperature frequency in fully developed laminar duct flows. *J. Eng. Phys. Thermophys*. **83**, 380-392.

[5] R. M. COTTA, M. D. MIKHAILOV, M. N. ÖZISIK. (1987). Transient conjugate forced convection in ducts with periodically varying inlet temperature. *Int. J. Heat Mass Transfer*. **30**, 2073-2082.

[6] D. M. BROWN, W. LI, S. KAKAC. (1993). Numerical and experimental analysis of unsteady heat transfer with periodic variation of inlet temperature in circular ducts. *Int. Comm. Heat Mass Transfer*. **20**, 883-899.

[7] B. FOURCHER AND K. MANSOURI. (1997). An approximate analytical solution to the Graetz problem with periodic inlet temperature. *Int. J. Heat Fluid Flow*. **18**, 229-235.

[8] K. MANSOURI AND A. HADIOUCHE. (2008). On the solution of a periodic internal laminar flow. *Proceedings of CHT-08 Int. Symp. on Advances in Computational Heat Transfer*.

[9] W. S. KIM AND M. N. ÖZISIK. (1989). Turbulent Forced Convection Inside a Parallel-Plate Channel With Periodic Variation of Inlet Temperature. *J. Heat Trans.-T. ASME*. **111**, 882-888.

[10] S. KAKAC AND W. LI. (1994). Unsteady turbulent forced convection in a parallel-plate channel with timewise variation of inlet temperature. *Int. J. Heat Mass Transfer 37*. **37**, 447-456.

[11] M. ARIK, C. A. A. SANTOS, S. KAKAC. (1996). Turbulent forced convection with sinusoidal variation of inlet temperature between two parallel-plates. *Int. Comm. Heat Mass Transfer* . **23**, 1121-1132.

[12] CUNLIANG LIU, JENS VON WOLFERSDORF, YINGNI ZHAI. (2014). Time-resolved heat transfer characteristics for steady turbulent flow with step changing and periodically pulsating flow temperatures. *Int. J. Heat Mass Transfer*. **76**, 184-198.

[13] CUNLIANG LIU, JENS VON WOLFERSDORF, YINGNI ZHAI. (2015). Comparison of time-resolved heat transfer characteristics between laminar and turbulent convection with unsteady flow temperatures. *Int. J. Heat Mass Transfer*. **84**, 376-389.

[14] CUNLIANG LIU, JENS VON WOLFERSDORF, YINGNI ZHAI. (2015). Time-resolved heat transfer characteristics for periodically pulsating turbulent flows with time varying flow temperatures. *Int. J. Thermal Sciences*. **89**, 222-233.

[15] R. J. MOFFAT. (1998). What's new in convective heat transfer? *Int. J. Heat and Fluid Flow*. **19**, 90-101.